

## Mechanisms of cell positioning during *C. elegans* gastrulation

Jen-Yi Lee and Bob Goldstein

Department of Biology, University of North Carolina, Chapel Hill, NC 27599, USA

Accepted 17 October 2002

### SUMMARY

Cell rearrangements are crucial during development. In this study, we use *C. elegans* gastrulation as a simple model to investigate the mechanisms of cell positioning. During *C. elegans* gastrulation, two endodermal precursor cells move from the ventral surface to the center of the embryo, leaving a gap between these ingressing cells and the eggshell. Six neighboring cells converge under the endodermal precursors, filling this gap. Using an in vitro system, we observed that these movements occurred consistently in the absence of the eggshell and the vitelline envelope. We found that movement of the neighbors towards each other is not dependent on chemotactic signaling between these cells. We further found that *C. elegans* gastrulation requires intact microfilaments, but not microtubules. The primary mechanism of microfilament-based motility does not appear to be through protrusive structures, such as lamellipodia or

filopodia. Instead, our results suggest an alternative mechanism. We found that myosin activity is required for gastrulation, that the apical sides of the ingressing cells contract, and that the ingressing cells determine the direction of movement of their neighboring cells. Based on these results, we propose that ingression is driven by an actomyosin-based contraction of the apical side of the ingressing cells, which pulls neighboring cells underneath. We conclude that apical constriction can function to position blastomeres in early embryos, even before anchoring junctions form between cells.

Movies available on-line

Key words: Cell migration, In vitro system, Gastrulation, Morphogenesis, Polarity, Actomyosin cytoskeleton, *C. elegans*

### INTRODUCTION

Cell rearrangement is essential in development. Although morphogenesis involving epithelial sheets has been a topic of extensive investigation (reviewed by Jacinto et al., 2001), the mechanisms that govern the movement of individual cells during development are less well characterized. Individual cell migrations, such as those exhibited by sea urchin primary mesenchyme cells during skeletogenesis (Ettensohn, 1991) and by ascidian notochord cells during notochord formation (Munro and Odell, 2002), play an important role in early embryos.

One of the key cell rearrangements during development is gastrulation, the process by which metazoan embryos internalize their future endoderm, resulting in proper positioning of the three germ layers – the endoderm, the mesoderm and the ectoderm. The mechanisms of gastrulation differ between animals, ranging from the simple to the complex. For example, in the nematode *Caenorhabditis elegans*, embryos internalize their endoderm by the ingression of only two cells (Sulston et al., 1983), whereas, in chick embryos, the process is complex, requiring the coordinated movement of entire tissues immediately followed by neurulation (Schoenwolf, 1991). Owing to its simplicity, the gastrulation process in *C. elegans* is particularly well suited to studying individual cell movement and positioning during development.

*C. elegans* development follows a precise program of cell divisions (Sulston et al., 1983). The one-cell embryo divides into the anterior cell AB, which gives rise to most of the nervous system and epidermis, while the posterior cell, P<sub>1</sub>, produces the endoderm, germline and most of the mesoderm (Fig. 1A). Among the descendents of P<sub>1</sub> are several important players in gastrulation: the endoderm precursors Ea and Ep, and their neighbors, the germline founder cell P<sub>4</sub>, and the granddaughters of MS, which produce primarily mesoderm (we use 'MSxx' to indicate any one granddaughter of MS). Gastrulation begins with the ingression of Ea and Ep towards the center of the embryo, leaving a space between the cells and the eggshell known as the ventral cleft. Meanwhile, MSxx and P<sub>4</sub> move towards each other and fill the ventral cleft (Fig. 1B,C) (Sulston et al., 1983). In the experiments described in this paper, we analyzed the displacement of the Ea and Ep cells relative to their immediate neighbors. For convenience, we refer to these movements alone as gastrulation, although these initial movements are followed by internalization of almost half of the cells in the developing embryo to complete the entire process of gastrulation (Sulston et al., 1983; Nance and Priess, 2002).

A major advantage of using *C. elegans* embryos to study cell rearrangement is the potential to combine the powerful tools of direct cell manipulation, cell biology and genetics. An in vitro culture system exists whereby the eggshell and vitelline envelope can be removed (which we refer to as

devitellinization), and the resulting naked embryos can be cultured in embryonic growth medium (Edgar, 1995). This *in vitro* system was previously used to dissect cell-cell signaling and cell fate determination (Goldstein, 1992; Shelton and Bowerman, 1996; Lin et al., 1998; Berkowitz and Strome, 2000), and is thus well suited to study many aspects of embryogenesis. Use of *in vitro* models in other animal systems, such as Keller explants of *Xenopus* embryos, has allowed detailed examination of morphogenetic movements at the cellular level (Wilson and Keller, 1991).

Despite the numerous advantages of using *C. elegans* to study morphogenesis, the mechanisms that underlie *C. elegans* gastrulation are unknown. The success or failure of gastrulation is often noted in characterizing mutants, but few studies have actually addressed the mechanistic requirements for gastrulation. Proper endoderm fate appears to be required for gastrulation, as mutations that prevent endoderm specification also result in a gastrulation-defective phenotype (reviewed by Maduro and Rothman, 2002). In addition, proper cell cycle length may also be essential, as early Ea/Ep division appears to prevent gastrulation (Schierenberg et al., 1980; Knight and Wood, 1998). Other factors, such as the formation of small blastocoel-like spaces, an apical-basal polarized distribution of PAR proteins, and an accumulation of myosin at the ventral sides of Ea and Ep might play roles in gastrulation (Nance and Priess, 2002), but their functional requirements have not been tested. Therefore, it is currently unclear what mechanisms control this important event.

In this study, we first asked if we could extend the *C. elegans* *in vitro* system to study morphogenetic movements during gastrulation. We also addressed the following questions. What are the mechanisms of cell movement? Is chemotaxis involved? What is the role of the cytoskeleton? What determines the direction of cell movement?

## MATERIALS AND METHODS

### Strains and worm maintenance

Nematodes were cultured and handled as described (Brenner, 1974). Unless indicated, experiments were performed with the wild-type N2 (Bristol) strain. The following mutant and reporter strains were used: EU855 *mom-2(or309) V/nT1[unc-?(n754) let-?(IV;V)*; BW1943 *gad-1(ct226) dpy-11(e224) (V)*; TH2, an  $\alpha$ -tubulin::GFP fusion construct driven by the *pie-1* promoter (Oegema et al., 2001); WH212 *unc-119(ed3); ojls4[actin::YFP unc-119(+)]*; and KK871 *PAR-2::GFP*. Strains were maintained at 20°C, except for the *gad-1* strain, which was maintained at 16°C, then shifted overnight to the restrictive temperature of 25°C to obtain affected embryos, and the transgenic strains, which were maintained at 25°C. Filming was performed at 20–23°C.

### Devitellinization and blastomere culture/isolation

Devitellinization and blastomere culture techniques were performed essentially as described (Edgar, 1995; Goldstein, 1992), with the following exceptions: 10% hypochlorite (Sigma) was used; the enzyme solution consisted of 3 units/ml chitinase (Sigma), 6.6 mg/ml chymotrypsin (Sigma) and 0.1% penicillin-streptomycin (Gibco); and the Edgar's Growth Medium (EGM, also called Embryonic Growth Medium) (Edgar, 1995) did not contain heavy metals. In cases where a mouth pipette and needle were insufficient for blastomere separation, a micropipette was pulled by hand over a flame and the uncut tip was laid down between blastomeres to separate them. In

most experiments, embryos were checked the next day for the presence of birefringent gut granules, an indicator of proper cell fate specification (Babu, 1974; Laufer, 1980). A small percentage of embryos did not make gut granules (~3% of all experiments), and these were not included in data analyses.

### 4-D videomicroscopy

Embryos with eggshells were placed in egg buffer on a 0.1% poly-L-lysine (Sigma) coated coverslip, inverted over a 3% agar pad, and sealed with petroleum jelly. Devitellinized embryos and isolated blastomeres were placed in 15  $\mu$ l EGM on a coverslip with clay feet at its corners and sealed with petroleum jelly. Images were acquired on a C2400-07 Hamamatsu Newvicon video camera (Hamamatsu Photonics) mounted on a Nikon Eclipse 800 microscope (Nikon Instrument Group). Time-lapse images were acquired at 1  $\mu$ m sections every 30 seconds using 4D Grabber, and subsequently analyzed with 4D Viewer (Integrated Microscopy Resource, University of Wisconsin, Madison).

### Quantification of cell movements

For timing measurements, the beginning of gastrulation movement was chosen by the frame in each movie where P<sub>4</sub> and MS<sub>xx</sub> began to move towards each other. Because there is a slight variation in cell cycle length from embryo to embryo, cell cycle lengths were normalized: the beginning of movement was expressed as a fraction of the length of each embryo's total Ea/Ep cell cycle. For angle quantification measurements, two different approaches were used because of a difference between wild-type and mutant embryos (see Results). In all cases, the angles were measured using a protractor, with the line joining the centers of the Ea and Ep cell nuclei as the (0°) reference point. A measurement was taken at the indicated initial time point, and that value was subtracted from the measurement at the final time point, to give the total movement. Means and standard deviations were calculated as described for circular distributions (Zar, 1999). Watson-Williams tests revealed significant differences between the four embryo types for the three approaches (see Table 1). Multiple comparisons were made using pair-wise Watson-Williams tests. This procedure is analogous to using an ANOVA to determine the main effect of embryo type followed by pair-wise *t*-tests for multiple means comparisons between the embryo types. (This type of procedure produces a real risk of type I errors but could not be avoided because post hoc means comparison tests for circular data have not been developed.) It is likely that our angle measurements of P<sub>1</sub> isolates are underestimates, as we measured movements in one plane of a multiplane movie, and cells sometimes moved partially along the z-axis (in or out of the x, y plane observed). For measurements of apical surface/length, lengths from the apical border of Ea/MS<sub>x</sub>(x) to Ep/P<sub>4</sub> were measured from time-lapse images using Metamorph software, where the measuring tool was calibrated to micrometers. Two timepoints were taken: the first was at P<sub>4</sub> birth and the second was taken 20 minutes later. Three independent measurements were taken from each embryo at each time point, and were then averaged together to obtain a representative number for each embryo. Six embryos from each treatment were analyzed.

### Laser permeabilization experiments

Embryos were dissected from hermaphrodites, transferred to washed, 0.1% poly-L-lysine coated coverslips, coated with Nile Blue or Trypan Blue (Sigma), and washed in egg buffer or EGM. After mounting, the coverslip was sealed on two opposing edges with petroleum jelly, allowing for transfer of liquids from one side of the coverslip to the other. Embryos were permeabilized by irradiating the Nile Blue or Trypan Blue particles with a few low-energy laser pulses using a VSL-337 nitrogen laser (2 mW, Laser Science) mounted on a Nikon Eclipse 800 microscope. In experiments with SynaptoRed (Novagen), also known as FM4-64, 10  $\mu$ g/ml SynaptoRed in EGM was washed in and the coverslip subsequently sealed. Confocal

imaging was performed at three minute intervals with a Zeiss LSM 410 microscope with an argon krypton laser. Embryos were imaged live. Cytoskeletal inhibitors were introduced at the desired stages by placing 10  $\mu$ l at one end of the unsealed coverslip and using a Kimwipe at the other to wick up the excess liquid. This was repeated three times to ensure delivery of the drug. In some experiments, the same procedure was repeated with egg buffer or EGM in order to wash the drug out of the solution. The following drugs were used: 5  $\mu$ g/ml cytochalasin D, 10  $\mu$ M latrunculin B, 50  $\mu$ M taxol and 10  $\mu$ M nocodazole. All drugs were diluted in DMSO and used at a final concentration of 1% DMSO in either egg buffer or EGM. To calculate rate of ingression, kymographs were made using NIH Image v. 1.62 software. A line was drawn through the Ep nucleus, and this line follows the same slice for the entire duration of the film. The result is a distance over time graph, measuring the rate of Ep nucleus ingression. For the kinase inhibitors ML-7, ML-9 and H-7 (Calbiochem), the drugs were not washed in, but already diluted in EGM at the concentrations noted in the text and in Fig. 7.

### Scanning electron microscopy

Blastomeres were cultured and allowed to develop to gastrulation stages. The cells were washed twice with simplified culture medium (SCM) (Goldstein, 1995). The embryos were then fixed, post-fixed and washed as previously described (Priess and Hirsh, 1986). Cells were placed on a 0.1% poly-L-lysine coated coverslip, and subsequently dehydrated through a series of graded ethanol washes (30%, 50%, 70%, 100%, 100%). Critical-point drying was performed using CO<sub>2</sub> as the transition solvent, and the coverslip was mounted on an aluminum stub and sputter coated to a thickness of 15 nm with 60:40 Au:Pd alloy on a Hummer X Sputtering System (Anatech). Samples were observed at an accelerating voltage of 20 kV and photographed using a Cambridge S200 SEM. Images were acquired using NIH Image software and processed with Adobe Photoshop software.

### Immunofluorescence

Blastomeres were cultured and allowed to develop to gastrulation stages. They were then washed twice with SCM, fixed with 4% paraformaldehyde (Electron Microscopy Sciences), and washed three times with PBT (phosphate-buffered saline with 1% Tween-20). For phalloidin, embryos were extracted with sonicated 0.5% Triton-X-100 for 5 minutes immediately following fixation. The following concentrations were used: 1:50 Alexa Fluor 488 Phalloidin (F-actin, Molecular Probes) and 1:500 mouse  $\alpha$ -phosphotyrosine (P-Tyr-102, Cell Signaling Technology). Alexa Fluor 488-conjugated goat anti-mouse secondary antibody was used at 1:1000 (Molecular Probes). Confocal images were obtained as described above. Epifluorescence imaging was attained with a Hamamatsu Orca II (model C4742-98) charge-coupled device camera mounted on a Nikon Eclipse E600FN. Adobe Photoshop software was used to process the images for publication.

### Fluorescent microsphere experiments

For each experiment, 0.2  $\mu$ m yellow-green fluorescent, carboxylate-modified latex microspheres (Molecular Probes) were freshly diluted 1:4 in SCM, sonicated for 1 minute and added to P<sub>1</sub> isolates in EGM. The microspheres and P<sub>1</sub> isolates were quickly mixed together using a mouth pipette for three minutes, after which the P<sub>1</sub> isolates were transferred through two washes of EGM. The microspheres attach non-specifically to protein surfaces (Wang et al., 1994). The isolates were placed in 2  $\mu$ l of EGM in one well of an eight-well slide (ICN), with the three surrounding wells also containing 2  $\mu$ l of EGM. A coverslip was gently placed over the four wells, and sealed with valap (1:1:1 vaseline, lanolin and paraffin). Simultaneous DIC and GFP time-lapse images were acquired every 30 seconds at three planes, 1-1.5  $\mu$ m apart, using a Hamamatsu Orca II (model C4742-98) charge-coupled device camera mounted on a Nikon Eclipse E600FN. The

Metamorph software package (Universal Imaging) was used for microscope automation, image acquisition and image analysis. DIC and GFP images were combined into one image for analysis. Microsphere movements were traced by hand onto transparencies, from the beginning to the end of gastrulation movements, or until the microspheres went out of plane. As both the microspheres and the cells were moving at this time, the tracing template position was adjusted at each time interval along with cell movement, to make it possible to discern microspheres that were moving faster relative to cell boundaries from those remaining stationary on a moving cell. Kymographs of bead movement on Ea and Ep were made using Metamorph software to confirm tracing data. Tracings were scanned into the computer as TIFF images and then re-drawn using Canvas software. For vector addition, each cell was divided up into quadrants, and vectors were added if quadrants contained more than three vectors. Microspheres along cell boundaries or those that did not move were not included in the calculations. All calculations were performed by decomposing the vectors into x and y components. To obtain the average velocities for the set of microspheres from each quadrant, we first took the average of the x and y components separately, then extrapolated the total distance the microsphere would be expected to move by multiplying the distance from the added vector by a time ratio (total time/observed time) to obtain the total, average distance for all vectors in that quadrant. Then, we converted the relative distances into  $\mu$ m and divided this total, extrapolated distance by the total gastrulation time (25.2 minutes) to obtain the average rate of movement. Angle/direction of movement was calculated by calculating the arctangent of (y/x).

### Blastomere recombination experiments

P<sub>1</sub> cells were isolated and allowed to develop in EGM. To rotate partial isolates relative to each other, P<sub>1</sub> isolates were first split at one of three cell boundaries. For Ea and Ep recombinations, Ea and Ep were separated ~5 minutes after division and recombined. For MSxx and P<sub>4</sub> recombinations, the MS or P<sub>3</sub> cell was separated from the rest of the isolate and recombined one cell division later, when E had divided into Ea and Ep. Although the partial P<sub>1</sub> isolates were not deliberately rotated, we refer to them as rotated because they were placed back in contact without regard for their original rotational orientations; examining centrosome positions has demonstrated that this procedure can randomize rotational orientations (Goldstein, 1995). The recombined P<sub>1</sub> isolates were mounted on coverslips and filmed as described above. Analysis of the direction of movement depended on whether MSxx and P<sub>4</sub> moved in the same plane or not. In all cases, MSxx and P<sub>4</sub> always moved towards the Ea/Ep boundary. If both cells moved in the same plane, the movement was either 0° (towards each other) or 180° (away from each other). If a cell moved in or out of plane, a reference cell was chosen (see Fig. 8) and the non-reference cell was estimated to move 45°, 90° or 135° off the axis of movement of the reference cell.

## RESULTS

### Gastrulation can occur in vitro

In *C. elegans*, gastrulation is initiated at the 26-cell stage by the ingression of the endoderm precursor cells, Ea and Ep (Sulston et al., 1983). As Ea and Ep leave the eggshell, a space appears between the E cells and the eggshell (Fig. 1B,C). Six wedge-shaped, neighboring cells converge over the ventral surface of the E cells: P<sub>4</sub>, three granddaughters of MS (MSpp, MSpa, MSap), ABplpa and ABplpp (Fig. 1D). From a lateral view, P<sub>4</sub>, the germline precursor cell, is adjacent to Ep on the posterior side, while MSxx, one granddaughter of the mesodermal precursor MS cell, is

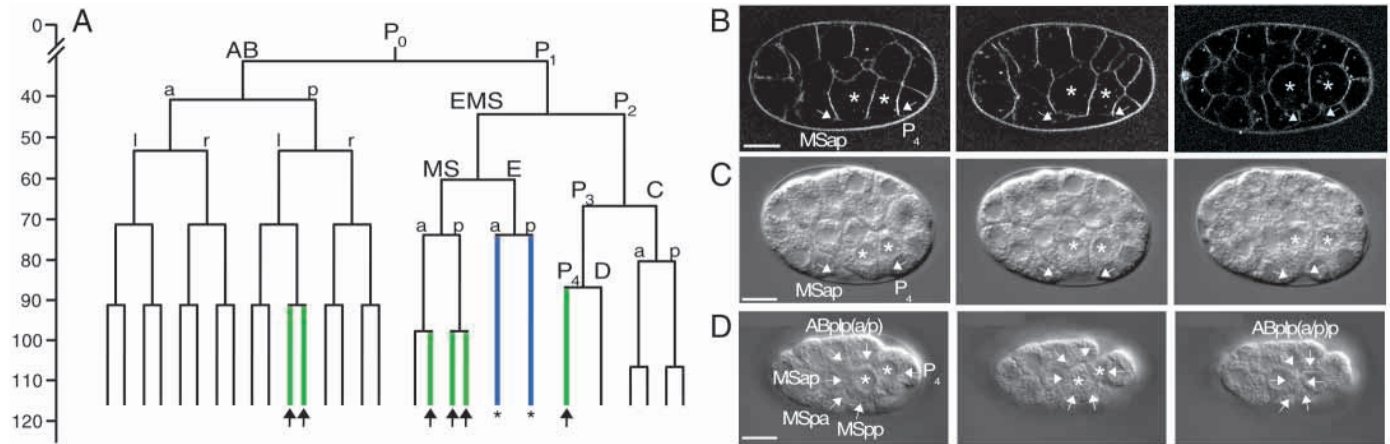


**Fig. 1.** *C. elegans* gastrulation. (A) Early embryonic lineage of *C. elegans* development. Daughters are annotated 'a' for anterior, 'p' for posterior, 'l' for left, and 'r' for right. Anterior is towards the left. The endoderm precursors, Ea and Ep, are labeled in blue. The neighboring cells that close the gastrulation cleft are in green (ABplpa, ABplpp, MSap, MSpa, MSpp and P<sub>4</sub>). The scale on the left refers to time, in minutes, since fertilization. (B) Confocal images of lateral view of gastrulating embryos labeled with the membrane marker SynaptoRed to better visualize cell boundaries. Ea and Ep ingress towards the center of the embryo, and are eventually surrounded by MSap and P<sub>4</sub>. Asterisks indicate Ea and Ep and neighboring cells are labeled with arrows in B-D. (C,D) Panels show DIC time-lapse views of gastrulation. (C) Lateral view of gastrulation, similar to B. Images are at 10 minute intervals. (D) Ventral view of gastrulation. From left to right, time intervals are 0, 12 and 32 minutes. As Ea and Ep 'sink' into the embryo, six cells close up the ventral cleft. Note that while ABplpa and ABplpp start moving toward the cleft, they divide and the posterior daughters of these cells finish the movement. In this and all figures, embryos are oriented anterior towards the left, and posterior towards the right. Scale bars: 10  $\mu$ m. Movies of time-lapse images are available online at <http://dev.biologists.org/supplemental/>.

adjacent to Ea on the anterior. P<sub>4</sub> and MSxx can be seen moving toward each other into the space left by the E cells, and they meet on the ventral side of Ea and Ep (Fig. 1B,C). Therefore, the ingression of Ea and Ep involves a total of eight cells, almost a third of the cells in the embryo at this stage. After this initial internalization of Ea and Ep, P<sub>4</sub> and the MS descendents ingress ~1 hour later, and gastrulation continues as additional cells ingress through the 300-cell stage (Nance and Priess, 2002). This internalization of Ea and Ep places the presumptive endoderm in the center of the embryo, as occurs in gastrulation in other organisms (Keller et al., 1991).

The *C. elegans* embryo develops inside a vitelline envelope, which is surrounded by a chitinous eggshell (Wood, 1988). It has previously been reported that gastrulation does not occur in devitellinized embryos, suggesting that the vitelline envelope might produce a micro-environment required for gastrulation (Schierenberg and Junkersdorf, 1992). However, half of the embryos cultured in that study did not make rhabditin/gut granules, a marker of endoderm differentiation in *C. elegans* embryos, suggesting that the embryonic culture medium used might not have supported development as well as EGM (see Materials and Methods).

To determine if gastrulation can occur in vitro, we devitellinized embryos, filmed their development in EGM, and compared them with intact embryos (Fig. 2A-H). Gastrulation movements occurred consistently in devitellinized embryos (Fig. 2E-H, six out of six embryos), and these movements occurred at the same time as they do in intact embryos (see below). Therefore, the eggshell and the vitelline envelope do not serve as required surfaces for gastrulation forces to act against or as sources for signals that are necessary for gastrulation to occur.

### Gastrulation does not require AB descendants

Gastrulation movements in the descendants of isolated P<sub>1</sub> cells were previously noted in some partial embryos (Lauer et al., 1980; Edgar, 1995). We wanted to extend what was observed by asking if these movements occur consistently in vitro, and to what extent the movements were similar to those seen in intact embryos. First, we tested whether gastrulation requires AB descendants, either as substrates for cell crawling or as a source of essential signals.

Time-lapse imaging of P<sub>1</sub> isolates showed that gastrulation movements occur consistently in vitro without AB descendants (Fig. 2I-P, 12/12 embryos). Without the eggshell or the AB descendants as reference points, we could not assess whether or not the E cells in the P<sub>1</sub> isolates were moving into what was once the center of the embryo. However, we always observed P<sub>4</sub> and MSxx moving towards each other, as they do in intact embryos (12/12 embryos), although not to the same extent (see below). The descendants of P<sub>1</sub> exhibited variable division patterns, producing partial embryos that ranged from a dumb-bell shape, in which the neighbors of the E cells made multiple cell-cell contacts with the E cells (Fig. 2I-L), to a linear orientation, in which there were single cell-cell contacts between the E cells and their neighbors (Fig. 2M-P). Partial embryos of all geometries underwent gastrulation movements (Fig. 2I-P). As we observed that both the leading and trailing edges of the neighboring cells were displaced in the direction of movement (data not shown), we infer that these are directed movements rather than cells simply spreading over the surfaces of Ea and Ep. Our results suggest that single cell-cell contacts between the E cells and their immediate neighbors, P<sub>4</sub> and MSxx, are sufficient for at least some gastrulation movements to occur.

Because P<sub>1</sub> isolates would enable us to perform cell

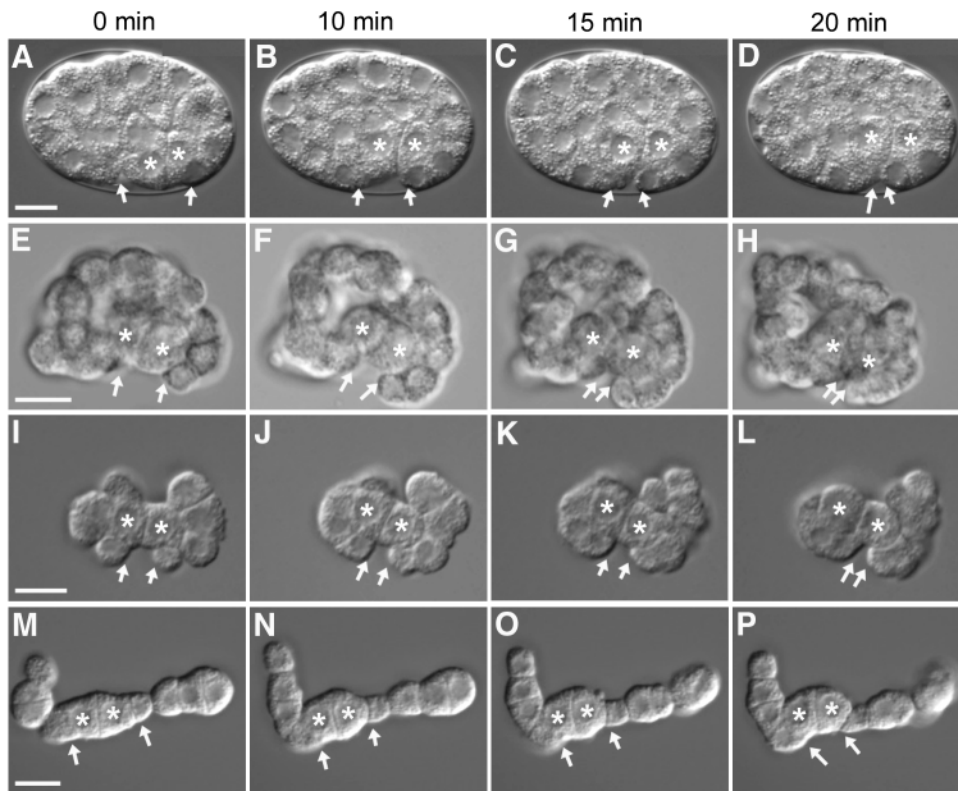


**Fig. 2.** Gastrulation in intact embryos, devitellinized embryos and P<sub>1</sub> isolates. Asterisks indicate Ea and Ep, arrows indicate MSxx and P<sub>4</sub>. Time-lapse images were time-standardized between all four sets, with 0 minutes indicating the start of gastrulation movements. (A-D) Time-lapse images of gastrulation in an intact embryo (same embryo as Fig. 1C), (E-H) in a devitellinized embryo, and (I-P) in P<sub>1</sub> isolates. Variation of starting orientation between intact and devitellinized embryos is due to devitellinization (A versus E). The two sets of P<sub>1</sub> isolate images represent two different division patterns, either in a dumb-bell orientation (I-L) or in a linear orientation (M-P). Linear orientation occurs in less than 10% of all P<sub>1</sub> isolates (data not shown). Other division patterns were variations between these two extremes. Scale bars: 10  $\mu$ m. Movies of time-lapse images available online at <http://dev.biologists.org/supplemental/>.

manipulations that are not feasible in intact, or even devitellinized, embryos, we were interested in determining to what extent gastrulation movements occurred normally in descendants of P<sub>1</sub> isolates. Thus, we next asked to what degree the movements we observed were similar to those in intact embryos in both the timing as well as the extent (distance) of the movements. In intact embryos, gastrulation always began after Ea and Ep were born, but before they divided (Fig. 3A, 10/10 embryos). Similarly, the onset of movements in both devitellinized embryos (six out of six embryos) and in P<sub>1</sub> isolates (12/12 embryos) always occurred before the end of the Ea/Ep cell cycle (Fig. 3A).

Next, we quantified the extent of movement by measuring the angle of movement of P<sub>4</sub> and MSxx relative to a reference axis defined by the positions of Ea and Ep nuclei (see Materials and Methods). As a negative control, we chose *mom-2* mutants, as gastrulation fails in embryos produced by *mom-2* mutant mothers (Rocheleau et al., 1997; Thorpe et al., 1997). *mom-2* mutants, like all gastrulation-defective mutants identified to date in *C. elegans* (Knight and Wood, 1998; Shi and Mello, 1998; Zhu et al., 1997; Tabara et al., 1999), have shortened Ea and Ep cell cycles, with Ea and Ep dividing about 15 minutes earlier than wild type. Therefore, as a time reference, we used the cell cycles of neighboring cells because those are not different in wild-type and *mom-2* embryos.

In wild-type, intact embryos, gastrulation movements can begin as early as P<sub>4</sub> birth (Fig. 3A). Because our measurements are affected by cell divisions, and because MSxx is born 12 minutes after P<sub>4</sub>, we first examined movement of P<sub>4</sub> during this 12 minute interval before MSxx birth. The amount of P<sub>4</sub> cell movement from all three wild-type groups (intact embryos, devitellinized embryos and P<sub>1</sub> isolates) was significantly

greater than that of P<sub>4</sub> movement in *mom-2* mutant embryos (Fig. 3B, Table 1).

Next, we examined the angle of movement by both P<sub>4</sub> and MSxx during the 30 minute period from when MSxx is born until it divides. MSxx moved significantly more in each of the wild-type groups than in P<sub>1</sub> isolates from *mom-2* mutant embryos (Fig. 3C, Table 1). Additionally, MSxx movement in another gastrulation-defective mutant, *gad-1* (Knight and Wood, 1998), was much less than in wild-type groups (data not shown). We were surprised to find that P<sub>4</sub> cells, during this time period, moved to a similar extent in both wild-type P<sub>1</sub> isolates and P<sub>1</sub> isolates derived from *mom-2* embryos. This result is not specific to *mom-2*, as analysis of *gad-1* produced a similar result (data not shown). The data suggests that the P<sub>4</sub> cells in these mutants may retain the ability to move or be translocated during this time period, or that the extent of P<sub>4</sub> movement in wild-type P<sub>1</sub> isolates is not as robust as that of MSxx movement.

We conclude that devitellinized embryos and P<sub>1</sub> isolates exhibit several aspects of gastrulation movements seen in intact embryos. First, the onset of movements occurs at the same time in intact embryos, devitellinized embryos, and in P<sub>1</sub> isolates. Second, the movements of P<sub>4</sub> and MSxx are always in the same direction as in intact embryos. Additionally, we found that in most cases, the extent of cell movement in wild-type P<sub>1</sub> isolates was significantly greater than that of gastrulation-defective mutant P<sub>1</sub> isolates. We note, however, that the extent of some cell movements in intact embryos is significantly greater than that in devitellinized embryos and in P<sub>1</sub> isolates (Table 1), suggesting that the eggshell, vitelline envelope and/or AB cells may be required for the full extent of gastrulation movements.

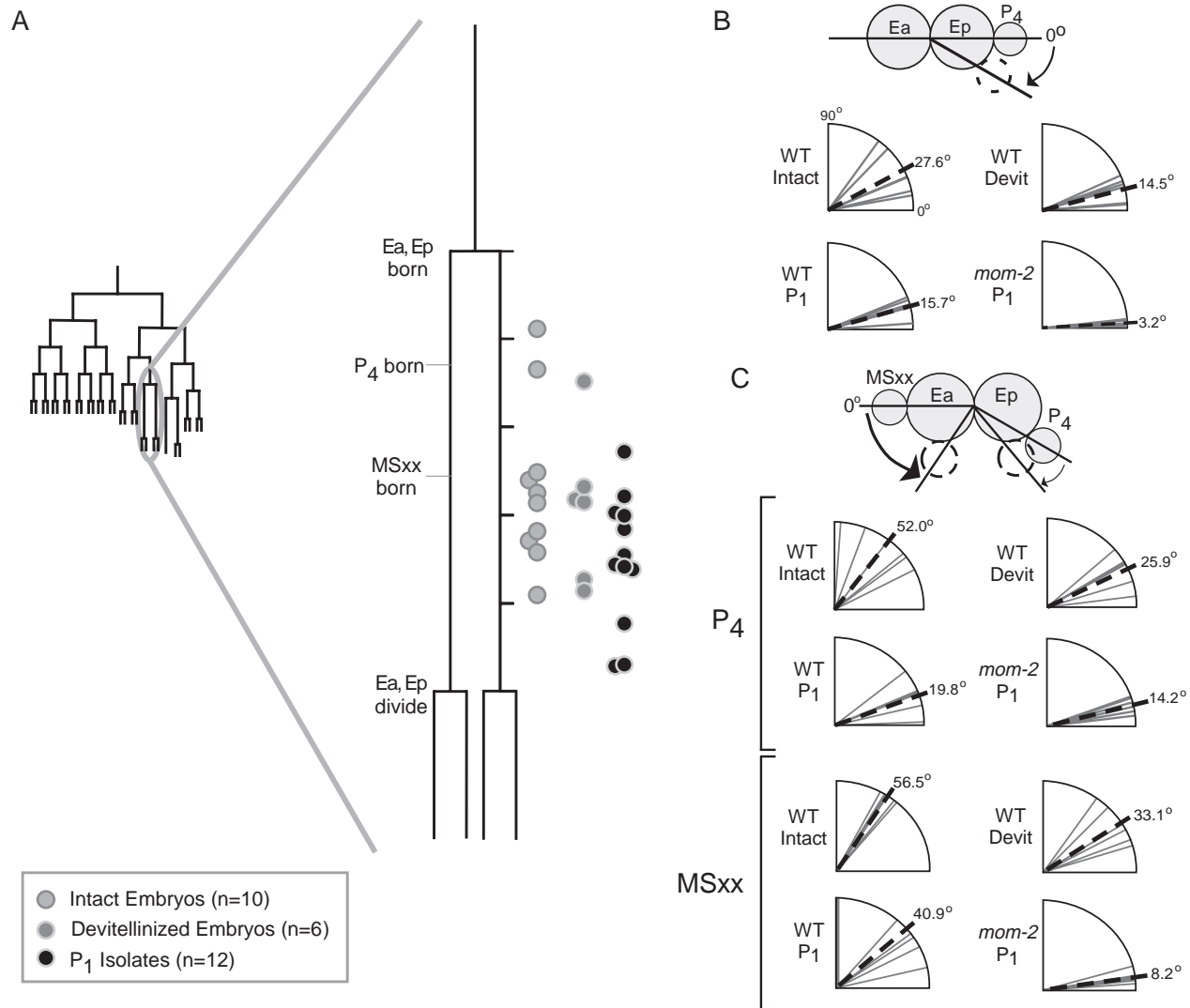


**Fig. 3.** Timing and extent of gastrulation movements. (A) Timing of the beginning of gastrulation movements in intact embryos (light gray circles), devitellinized embryos (medium gray circles) and P<sub>1</sub> isolates (black circles) with respect to the length of the Ea and Ep cell cycle. The timing of gastrulation was normalized between embryos (see Materials and Methods). Black ticks along Ea/Ep lineage represent a fifth of the total cell cycle. The early lineage is shown for reference. (B,C) Quantification of P<sub>4</sub> and MSxx movement relative to Ea and Ep in wild-type (WT) intact, devitellinized, P<sub>1</sub> isolates and *mom-2* P<sub>1</sub> isolates. The data are shown by quadrant graphs, with gray unbroken lines representing individual cases and black broken lines representing the mean for all embryos. A diagram representing the measurement method is shown above the graphs. (B) Quantification of P<sub>4</sub> movement relative to Ea and Ep from the time P<sub>4</sub> is born until MSxx is born (12 minutes). (C) Quantification of MSxx and P<sub>4</sub> movement relative to Ea and Ep after MSxx is born (30 minutes).

### MSxx does not chemotax towards P<sub>4</sub>

It is possible that P<sub>4</sub> and MSxx send chemotactic signals that could be used as cues to move towards each other. We tested this hypothesis by removing the potential sources of chemoattractants. Either MS or P<sub>2</sub> (the grandparents of MSxx and P<sub>4</sub>) were removed from P<sub>1</sub> isolates, and the truncated isolates were subsequently filmed to document cell movements in the manipulated embryos. When we removed P<sub>2</sub>, MSxx appeared to move as it would in unmanipulated P<sub>1</sub> isolates (Fig. 4D-F). Analysis with angle measurements confirmed this observation, as the average extent of movement of MSxx in truncated isolates was similar to that found in normal P<sub>1</sub> isolates (Fig. 4H) and was significantly greater than the movement seen in *mom-2* P<sub>1</sub> isolates (Table 1). Although we

also observed movement by P<sub>4</sub> after removing MS, the movement was not significantly greater than that in gastrulation-defective mutants, or significantly less than that in wild-type P<sub>1</sub> isolates (Table 1). Therefore, we cannot make a conclusion for P<sub>4</sub> on the basis of this experiment alone. We conclude that MSxx does not rely on a chemotactic signal from P<sub>4</sub> during gastrulation.

### Intact microfilaments are required for gastrulation

As the cytoskeleton plays a central role in cell motility, we asked whether microtubules and/or microfilaments were required for gastrulation. To test this, we permeabilized intact, gastrulating embryos by laser ablating holes in the eggshell and then exposed the embryos to various cytoskeletal inhibitors.

**Fig. 4.** MSxx and P<sub>4</sub> do not chemotax towards each other during gastrulation. Asterisks indicate Ea and Ep, an 'X' indicates the removed cells, and the remaining neighbor is labeled with an arrow.

(A-C) P<sub>4</sub> moves with respect to Ea and Ep in the absence of MS. (D-F) MSxx moves with respect to Ea and Ep in the absence of P<sub>4</sub>. (G) Angle quantification of six sets of

each manipulation, as in Fig. 3. The angle measurements for P<sub>4</sub> represent only the first 12 minutes of movement, as this number was significant from *mom-2* P<sub>4</sub> (see Results, Table 1). Scale bars: 10  $\mu$ m.

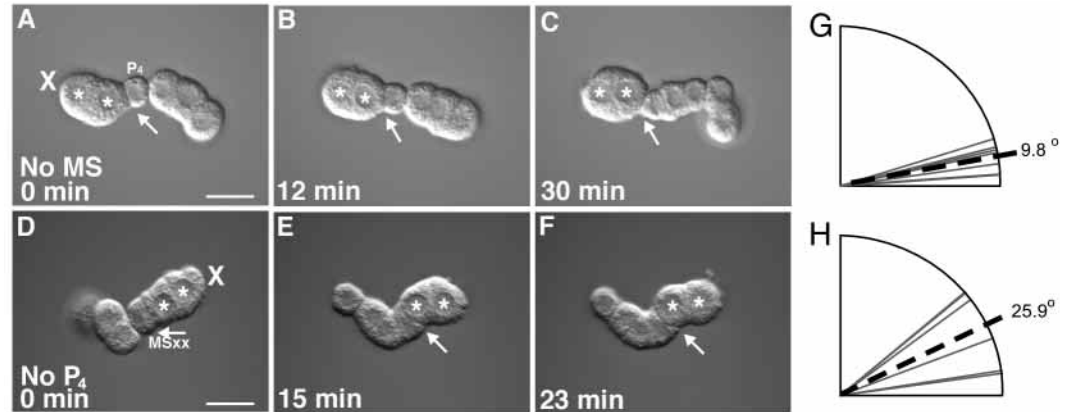


**Table 1. Angle measurements in intact embryos, devitellinized embryos and P<sub>1</sub> isolates**

Genotype	Manipulation	Average movement (degrees, $\pm$ s.d.)			n
		P <sub>4</sub> (first 12 minutes)*	P <sub>4</sub> (30 minutes) <sup>†</sup>	MSxx (30 minutes)	
Wild-type (N2)	Intact	27.6 ( $\pm$ 16.9) <sup>‡</sup>	52.0 ( $\pm$ 20.4) <sup>§</sup>	56.5 ( $\pm$ 3.9) <sup>††</sup>	6
	Devitellinized	14.5 ( $\pm$ 7.5) <sup>‡</sup>	25.9 ( $\pm$ 10.9) <sup>¶, **</sup>	33.1 ( $\pm$ 13.4) <sup>††, **</sup>	6
	P <sub>1</sub> isolate	15.7 ( $\pm$ 5.7) <sup>‡</sup>	19.8 ( $\pm$ 10.9) <sup>¶, **</sup>	40.9 ( $\pm$ 24.1) <sup>††</sup>	6
<i>mom-2(or139)</i>	P <sub>1</sub> isolate	3.17 ( $\pm$ 1.8)	14.17 ( $\pm$ 4.7)	8.16 ( $\pm$ 3.4)	6
Wild-type (N2)	EMS (no P <sub>2</sub> )	NA	NA	25.9 ( $\pm$ 14.0) <sup>††</sup>	6
	E+P <sub>2</sub> (no MS)	9.83 ( $\pm$ 4.9) <sup>‡</sup>	19.9 ( $\pm$ 12.0) <sup>¶</sup>	NA	7

\*The time period between P<sub>4</sub> birth and MSxx birth.

<sup>†</sup>The time of MSxx birth until MSxx division. For the range of numbers, see Fig. 3B and Fig. 4G,H.

Differences between wild-type groups in each time period were not significantly different from each other, except in cases indicated by \*\*, where differences were seen between devitellinized embryos or P<sub>1</sub> isolates compared to intact embryos. No significant differences were seen between devitellinized embryos and P<sub>1</sub> isolates.

n, number of cases; NA, not applicable.

<sup>‡</sup>*P*<0.025 versus *mom-2* P<sub>1</sub> isolate P<sub>4</sub>, first 12 minutes.

<sup>§</sup>*P*<0.05 versus *mom-2* P<sub>1</sub> isolate P<sub>4</sub>, 30 minutes.

<sup>¶</sup>*P*>0.05 versus *mom-2* P<sub>1</sub> isolate P<sub>4</sub>, 30 minutes.

<sup>††</sup>*P*<0.025 versus *mom-2* P<sub>1</sub> isolate MSxx.

Exposing the embryos to taxol, which suppresses microtubule dynamics in living cells (Yvon et al., 1999), or to the microtubule-destabilizing drug nocodazole, had the expected effects on microtubule distribution in gastrulating embryos, but neither drug prevented gastrulation (Fig. 5A-C). We conclude that microtubules do not play an essential role specifically during *C. elegans* gastrulation in producing movements.

By contrast, all embryos subjected to the microfilament assembly inhibitors cytochalasin D or latrunculin B did not gastrulate (Fig. 5E,F), suggesting that intact microfilaments are required for gastrulation. Examination of the actin distribution following drug treatment confirmed that actin microfilaments were no longer cortically enriched following treatment (Fig. 5E,F). To determine whether microfilaments are required only for gastrulation to initiate, or also for cells to continue moving, we exposed embryos to cytochalasin D during the middle of gastrulation, when MSxx and P<sub>4</sub> were about halfway towards meeting each other. Gastrulation halted immediately upon exposure to the drug (six out of six embryos). To ensure that cytochalasin D was not simply killing the embryos, we performed washout experiments to test the reversibility of the drug. Upon washout of cytochalasin D, gastrulation consistently resumed, after an

average of 11 $\pm$ 6 minutes (15/15 embryos). In addition, when we examined the rate of movement, we confirmed that during cytochalasin D treatment, the E cells did not ingress (Table 2). After washout, the rate of Ea/Ep movement was roughly equivalent to untreated control embryos (Table 2). Therefore, intact microfilaments are required throughout *C. elegans* gastrulation.

### Cells do not appear to move via a classical crawling mechanism

Actin-dependent mechanisms of motility mediated by cell protrusions are well documented in other motility systems, such as growth cones, keratocytes and fibroblasts (Mitchison and Cramer, 1996). We were interested in whether gastrulating cells in *C. elegans* also move by a similar mechanism. Crawling cells typically send out actin-rich protrusions, in the form of filopodia or lamellipodia, towards the direction of movement. Actin polymerization at the leading edge of the cell, in combination with traction at the cell base, results in forward displacement of the cell body. Simultaneously, the cortex and cell surface move rearward relative to the direction of movement. Finally, the very rear of the cell must de-adhere from the substrate so that there is a total forward motion of the

**Fig. 5.** Microfilaments are required for gastrulation. Asterisks indicate Ea and Ep. Confocal imaging of live embryos documents the qualitative, not quantitative, effects of pharmacological agents on tubulin and actin distribution. (A-C) Effects of drugs on tubulin in live embryos expressing Tubulin::GFP strain, treated with (A) 1% DMSO (control), (B) 50  $\mu$ M taxol and (C) 10  $\mu$ M nocodazole. (D-F) Effects of drugs on actin in live embryos expressing Actin::YFP, treated with (D) 1% DMSO, (E) 5  $\mu$ g/ml cytochalasin D and (F) 10  $\mu$ M latrunculin B. 1% DMSO treatment was the control as this was the final concentration of DMSO used for the drug studies. Gastrulation progressed normally in the presence of 1% DMSO. To the right of each image are the numbers of embryos assayed for gastrulation. The embryos imaged were different from those used for the assay. Scale bar: 10  $\mu$ m.

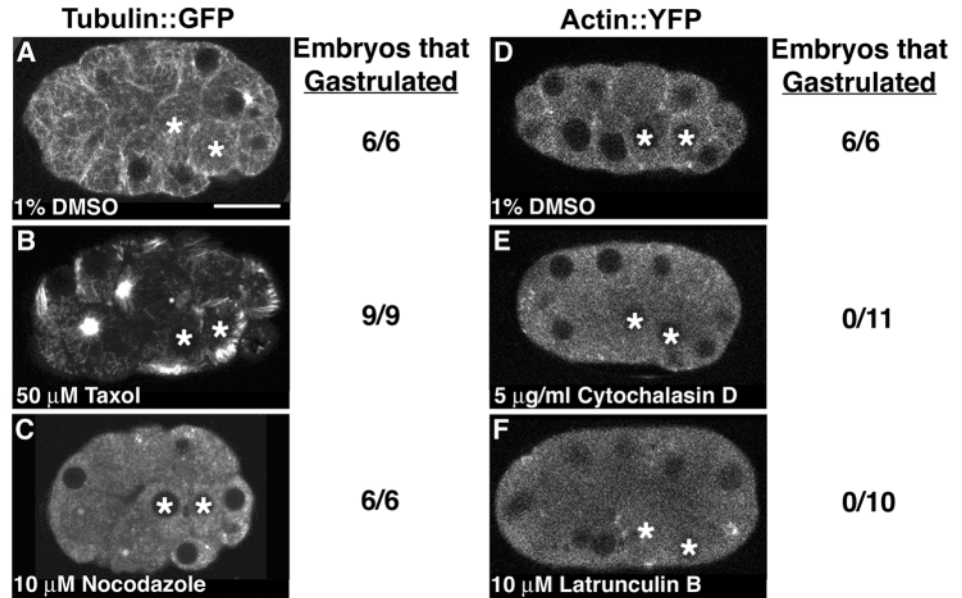


**Table 2. Rate of Ea/Ep ingression following cytochalasin D treatment**

Treatment	Average movement ( $\mu$ m/minute $\pm$ s.d.)		n
	During drug exposure	After washout/during gastrulation	
Control	NA	0.227 ( $\pm$ 0.067)	3
Cytochalasin D	-0.095 ( $\pm$ 0.082)	0.281 ( $\pm$ 0.055)	3

Rates were calculated from kymographs (see Materials and Methods). The time window measured started at the ingression of Ea and Ep and ended with their division. Positive numbers indicate movement in the direction of the center of the embryo. Slower movement in the opposite direction occurs in cytochalasin D as cells lose their shape.

cell (Mitchison and Cramer, 1996). In the case of gastrulation, Ea and Ep could be actively migrating towards the center of the embryo, or the neighboring cells could be crawling towards each other, using Ea and Ep as a substrate.

We used several independent methods to test if cells were indeed crawling via actin-mediated protrusions. Our initial approach was to look for extensions or cell shape changes in gastrulating P<sub>1</sub> isolates. Tracings of the cell shapes from time-lapse images during the time of gastrulation showed that P<sub>4</sub> and MSxx exhibited subtle cell shape changes at the leading edge towards the direction of movement, while Ea and Ep did not make any such observable shape changes (data not shown). This suggested that P<sub>4</sub> and MSxx might be making extensions and crawling towards each other, using the E cells as substrates. To test this, we used scanning electron microscopy (SEM) to investigate whether or not the cells produced extensions. Examination of both devitellinized embryos and P<sub>1</sub> isolates by SEM showed no consistent evidence of filopodia or lamellipodia (intact,  $n=8$ , data not shown; P<sub>1</sub> isolates,  $n=9$ , Fig. 6A). In some cases (four out of eight intact embryos, two out of nine P<sub>1</sub> isolates), we saw flattened protrusions at cell boundaries reminiscent of those reported previously in devitellinized embryos (Nance and Priess, 2002). However, there was never more than one cell per embryo exhibiting a protrusion and the cell that exhibited the protrusion varied from

embryo to embryo. In another approach, we reasoned that if the cells had actin-rich extensions, then we should see an increased intensity of filamentous actin (F-actin) at the leading edge of the motile cells. Staining P<sub>1</sub> isolates with fluorescent phalloidin, which marks F-actin, did not reveal an enrichment of actin at any specific cell-cell boundary ( $n=8$ , Fig. 6B). Another marker of active protrusions is phosphotyrosine, which has been shown to be enriched at the leading edge of crawling cells including nematode sperm and *Aplysia* growth cones (Italiano et al., 1996; Wu and Goldberg, 1993). We observed no polarized enrichment of phosphotyrosine at any specific cell-cell leading edge ( $n=12$ , Fig. 6C, and legend). We also used PAR-2::GFP as a live cortical marker in P<sub>4</sub> (Boyd et al., 1996) and found that the cortex of the P<sub>4</sub> cell did not make protrusions as it moved over the ventral surface of Ep (data not shown). Finally, tracking the surfaces of cells with fluorescent markers showed that the surface of MSxx does not move rearwards relative to the movement of the cell body, as would be expected from protrusion based crawling (see below). Together, these approaches suggest that cells do not form lamellipodia or filopodia and are unlikely to move via protrusions during *C. elegans* gastrulation.

### Myosin is required for cell movement

If cells do not move via protrusion-based cell crawling, then they must either move through another microfilament-dependent process, or microfilaments must play an indirect role in movement. Recent evidence showed an accumulation of NMY-2, a non-muscle myosin type II, at the ventral cortex of Ea and Ep during gastrulation (Nance and Priess, 2002), but whether or not this accumulation was required for gastrulation was not tested. Therefore, we asked if myosin activity was required for gastrulation.

As loss of NMY-2 results in severe defects in establishment of polarity and in execution of cytokinesis very early in embryogenesis, before gastrulation (Guo and Kemphues, 1996), we tested the role of myosin activity using ML-7, a potent and specific inhibitor of myosin light chain kinase (Saitoh et al., 1987). As ML-7 has not been used previously in *C. elegans*

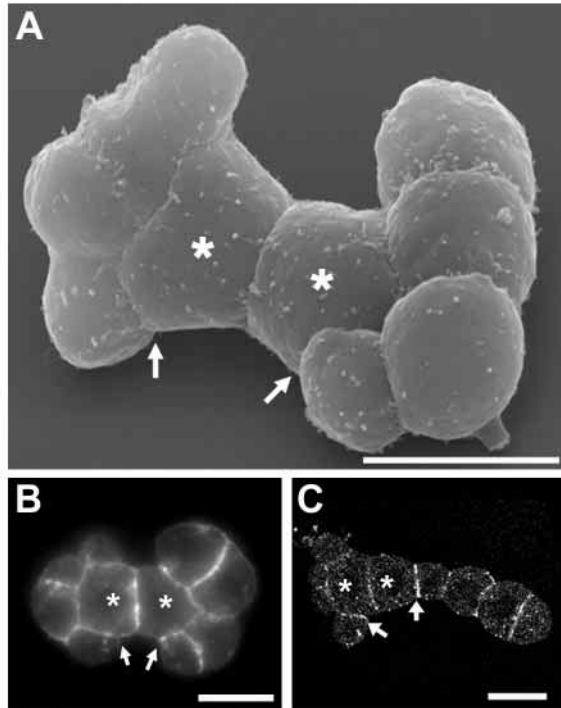


**Fig. 6.** No lamellipodia or filopodia form in P<sub>1</sub> isolates. Ea and Ep are labeled with asterisks, and arrows indicate presumptive leading edges of MSxx and P<sub>4</sub>. (A) Scanning electron micrograph of a P<sub>1</sub> isolate. (B) F-actin localization. (C) Phosphotyrosine localization. An enrichment of phosphotyrosine was seen at the Ep/P<sub>4</sub> boundary, but is unlikely to be functionally significant as it was not polarized in the direction of movement and it was not present at the Ea/MSxx boundary. Additionally, it was recently shown that phosphotyrosine accumulates at the EMS/P<sub>2</sub> boundary due to a signaling pathway that is not implicated in gastrulation (Bei et al., 2002). Scale bars: 10  $\mu$ m.

embryos, we performed dose response experiments to test the specificity of the effect of ML-7 and two related compounds, ML-9 and H-7, on gastrulation. ML-9 is also a MLCK inhibitor, but has ten-times less affinity for MLCK compared with the affinity of ML-7, whereas H-7 is a specific inhibitor of PKA, but exhibits a very weak affinity for myosin light chain kinase (Saitoh et al., 1987; Mabuchi and Takano-Ohmuro, 1990). We found that while 250  $\mu$ M ML-7 was sufficient to completely inhibit gastrulation, 750  $\mu$ M ML-9 and 4 mM H-7 were required to inhibit gastrulation (Fig. 7). We also found that exposure of embryos to 250  $\mu$ M ML-7 immediately halted cell movement at the beginning of gastrulation (six out of six embryos), as well as in the middle of gastrulation (seven out of seven embryos). 750  $\mu$ M H-7 was insufficient to inhibit gastrulation, but these embryos arrested early, before morphogenesis, suggesting other, potentially PKA-dependent defects (seven out of seven embryos). These experiments suggest that ML-7 specifically inhibits MLCK in *C. elegans* embryos and that myosin activity is required for cell movements throughout *C. elegans* gastrulation.

#### Cell surface tracking shows evidence of cell contraction

Our experiments with pharmacological agents suggest that actin and myosin play an essential role in *C. elegans*

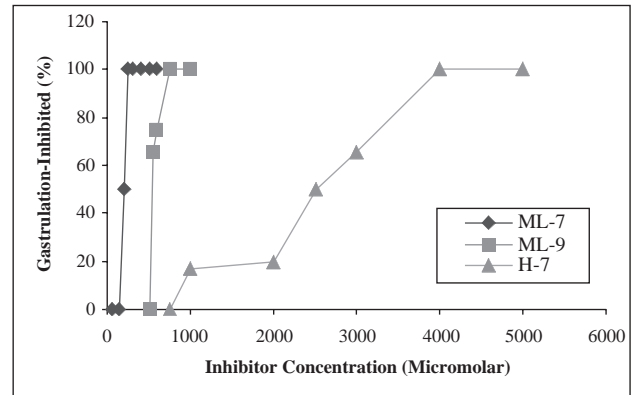


**Fig. 7.** ML-7 and ML-9, myosin light chain kinase inhibitors, are more potent inhibitors of gastrulation than H-7, a PKA inhibitor. Embryos were assayed as gastrulation-inhibited if the ventral surfaces of Ea and Ep were not fully covered by P<sub>4</sub> and MSxx by 1 hour after exposure to inhibitor. Ki (inhibition coefficient, expressed in  $\mu$ M) of the drugs against MLCK are as follows: ML-7, 0.3; ML-9, 3.8; H-7, 97 (Mabuchi and Takano-Ohmuro, 1990). We found that the doses required to completely inhibit gastrulation were as follows: ML-7, 250  $\mu$ M; ML-9, 750  $\mu$ M; H-7, 4 mM. We note that as much as 300  $\mu$ M was required to inhibit MLCK in *Xenopus* growth cones (Ruchhoeft and Harris, 1997), and high concentrations may be required to out-compete the reservoir of endogenous ATP, as both ML-7 and ML-9 are ATP analogs (Saitoh et al., 1987). Each data point represents between four and 13 embryos.

gastrulation, but the mechanism of movement is still unclear. One possible mechanism is that MSxx and P<sub>4</sub> could be actively moving via a rotating mechanism, where the cells would roll like wheels towards each other onto the ventral sides of Ea and Ep, possibly mediated by local gradients in cell adhesion. An alternative model is that a ventral, actomyosin-based contraction toward the Ea and Ep border drives the neighboring cells closer together. One prediction of this model is that the apical (ventral) surfaces of Ea and Ep should decrease in size during gastrulation, while embryos treated with the myosin inhibitor would not. We therefore measured the distance along the apical surface between the Ea/MSxx(x) border and the Ep/P<sub>4</sub> border (see Materials and Methods). We found that untreated, control embryos underwent an average apical reduction of 7.7 ( $\pm$ 2.3)  $\mu$ m during gastrulation, whereas the apical surfaces of embryos treated with ML-7 was reduced by 1.1 ( $\pm$ 2.3)  $\mu$ m during the same time frame. Therefore, the apical surface areas of Ea and Ep decrease during gastrulation, while myosin-inhibited embryos do not undergo significant changes.

Although these measurements are consistent with the contraction model, they are also consistent with models in which cells roll and also with models where the apical surfaces decrease as a result of basolateral expansion. To assess directly how cell surfaces behave, we tracked the surfaces of cells with fluorescent microspheres and filmed them during gastrulation. Fluorescent microspheres are useful markers for tracing the movement at the cell surface because they do not become engulfed by cells and are relatively photostable (Wang et al., 1994). Thus, if Ea and Ep were undergoing actomyosin contraction, then the microspheres on the ventral cortex of Ea and Ep would converge toward the Ea/Ep boundary. However, if the neighboring cells were rotating, then the microspheres

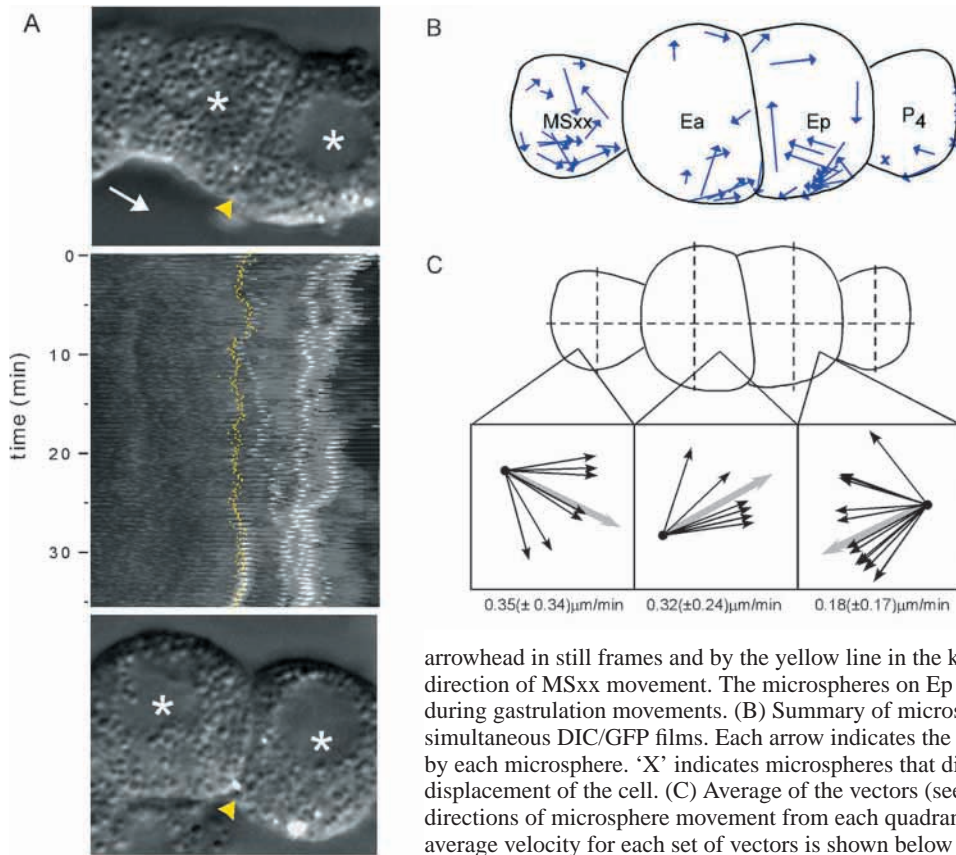


**Fig. 8.** Microsphere-marking of cell surfaces reveals that the ventral surfaces of Ea and Ep contract during gastrulation. (A) Kymograph derived from movements of microspheres (white) during gastrulation from one film of a wild-type P<sub>1</sub> isolate. In the kymograph, the image in each frame of the time-lapse recording is used to generate horizontal lines of image data that are pasted together in descending order; hence, time is represented on the y-axis. Each pixel in a horizontal line of image data was created by selecting the brightest pixel in a 20-pixel high region. As a result, horizontal movement of microspheres can be seen as horizontal movement of white dots as the kymograph proceeds from top to bottom. First frame and last frame used for the kymograph are above and below the kymograph, respectively. Ea and Ep are labeled with asterisks, the Ea/Ep boundary is marked by yellow

arrowhead in still frames and by the yellow line in the kymograph, and the white arrow indicates the direction of MSxx movement. The microspheres on Ep can be seen converging towards each other during gastrulation movements. (B) Summary of microsphere movements traced from all ten simultaneous DIC/GFP films. Each arrow indicates the total displacement and angle of movement by each microsphere. 'X' indicates microspheres that did not exhibit any displacement relative to the displacement of the cell. (C) Average of the vectors (see Materials and Methods). Insets show the directions of microsphere movement from each quadrant, with the average direction in gray. The average velocity for each set of vectors is shown below the box.

on the neighboring cell surfaces would be displaced in the direction of movement. Finally, if Ea and Ep were basolaterally expanding, then the beads on the apical surface of Ea and Ep should either remain stationary or move slightly away from the Ea/Ep boundary.

Partial embryos were incubated with microspheres, and a large number of microspheres were observed on the ventral surfaces of Ea, Ep and MSxx; whether or not this distribution is nonrandom and reflective of an increased degree of adhesivity at these surfaces is unclear. As these surfaces had a sufficiently large number of microspheres, we limited our analysis to these surfaces. We found that microspheres on the ventral sides of Ea and Ep generally moved toward the Ea/Ep boundary (Fig. 8). We also observed microspheres on the ventral side of MSxx moving along the cell surface towards Ea (Fig. 8). These results are consistent with the model that the ventral sides of Ea and Ep contract, and that MSxx might additionally contribute to movement by rotating towards Ea during gastrulation.

### Polarity in Ea and Ep dictates the direction of movement of neighboring cells

The observations that P<sub>4</sub> and MSxx move toward each other in P<sub>1</sub> isolates, that a non-muscle myosin is enriched in the ventral side of Ea and Ep (Nance and Priess, 2002), that myosin activity is required for gastrulation and that the ventral sides of Ea and Ep contract during gastrulation suggest that Ea and Ep may be ingressing via a myosin-based contraction of their ventral surfaces. One prediction of this hypothesis is that Ea

and Ep should be capable of dictating the direction of movement of their neighbors, regardless of the orientation of the neighbors. To test this, we rotated cells relative to each other by bisecting a P<sub>1</sub> isolate at various cell boundaries, recombining the isolated halves, and filming the partial embryos to document the ensuing direction of movement (see Materials and Methods, Fig. 9). We tested three variations of rotation experiments, in which we separated and recombined P<sub>1</sub> isolates at the Ea and Ep, Ea and MSxx, or Ep and P<sub>4</sub> boundaries.

We found that when we separated and recombined Ea and Ep, MSxx and P<sub>4</sub> did not move towards each other in the same axis as they did in unmanipulated P<sub>1</sub> isolates. Instead, the cells moved toward the Ea/Ep boundary in a range of directions relative to each other (Fig. 9A). Thus, when Ea/Ep orientation was randomized, so was the direction of movement by MSxx and P<sub>4</sub>. In addition, because the neighbors move in different directions, this result further confirms that MSxx and P<sub>4</sub> are not chemotaxing towards each other.

In isolates where MSxx and Ea were separated and recombined, MSxx always moved in the same direction as P<sub>4</sub> (10/10 embryos; Fig. 9B). Similarly, in most cases, P<sub>4</sub> moved in the same direction as MSxx where P<sub>4</sub> had been recombined with Ep (seven out of ten embryos; Fig. 9C). Curiously, in a small number of Ep/P<sub>4</sub> recombination cases, the neighboring cells moved in the same plane toward each other, but in the opposite direction (three out of ten embryos; Fig. 9C). It is possible that P<sub>4</sub> may influence the orientation by which polarity is established in Ep, although this has not been tested. We

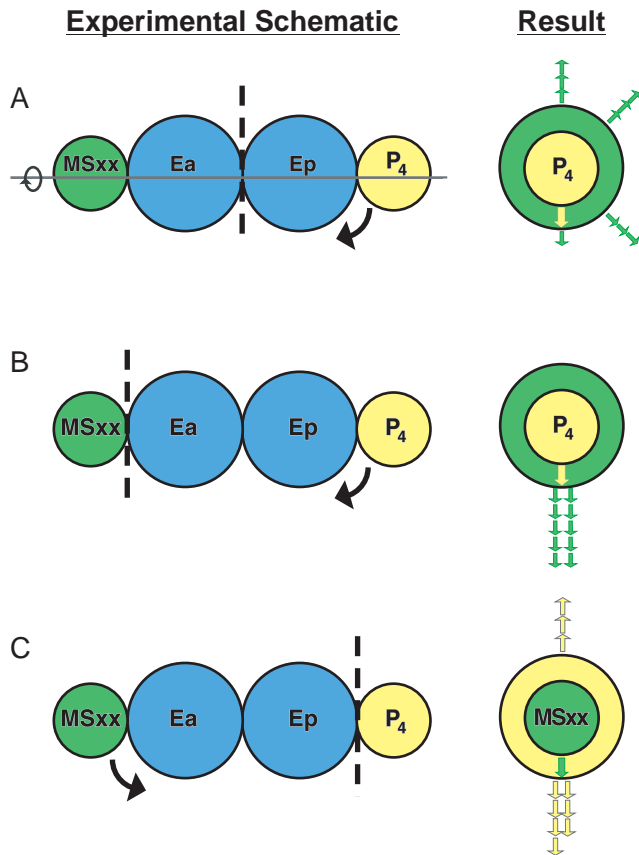


**Fig. 9.** Ea and Ep polarity directs the movement of their neighbors. On the left side of each panel is a schematic drawing of part of a P<sub>1</sub> isolate and the experiment performed. Cells in the isolates were separated at the site indicated by the broken line, rotated along an axis (unbroken gray line in A), and recombined in their normal orientations. The arrow below the cells indicates the direction of cell movement by the reference cell. On the right of each panel is the corresponding side view, in which the P<sub>1</sub> isolates are oriented as if looking down from one end, either P<sub>4</sub> or MSxx (as indicated). Yellow arrows indicate the direction of movement of P<sub>4</sub> cells and the green arrows indicate the direction of movement of MSxx cells. Separation and recombination of (A) Ea and Ep, with P<sub>4</sub> as the reference cell; (B) MSxx and Ea, with P<sub>4</sub> as the reference cell; or (C) P<sub>4</sub> and Ep, with MSxx as the reference cell.

conclude that Ea and Ep are polarized in a way that can generally dictate the direction of movement of their neighbors.

## DISCUSSION

### Mechanism of movement in *C. elegans* gastrulation

Our results suggest a mechanism for cell movement during *C. elegans* gastrulation, whereby an actomyosin-based contraction constricts the ventral surfaces of the endodermal precursor cells, pulling neighboring cells underneath and resulting in internalization of the future endoderm (Fig. 10). As all of the neighboring cells, regardless of their orientations, move towards the ventral surface of the ingressing cells (Fig. 9), and as beads placed on the ingressing cells will move in this direction (Fig. 8), we speculate that ventral contraction of

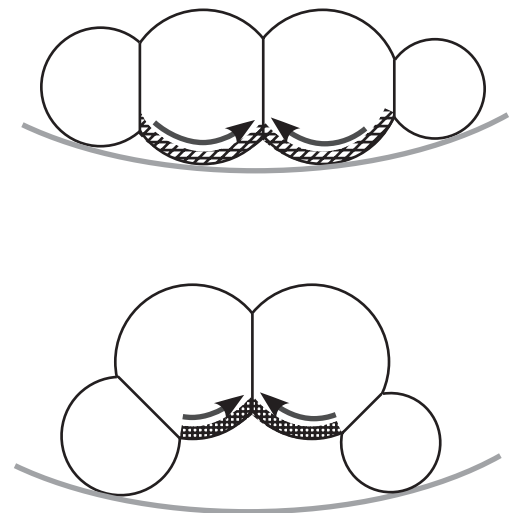


**Fig. 10.** Model of cell contraction during *C. elegans* gastrulation. (Top) Ea and Ep with myosin enriched at the ventral side. Hatching represents myosin, while gray arc underneath the cells represents the eggshell. Myosin-based contraction causes the ventral side of Ea and Ep to constrict, bringing neighbors closer to each other, which pushes Ea and Ep into the center of the embryo (bottom).

the ingressing cells is sufficient to move the neighboring cells. Given that enrichments of NMY-2 have been observed at the ventral side of other cells that ingress later in gastrulation (Nance and Priess, 2002), it is tempting to speculate that this same mechanism is used repeatedly to internalize cells in the *C. elegans* embryo.

Additional mechanisms may contribute additively or redundantly to ventral contraction of Ea and Ep. There are indications that some neighboring cells may make an active contribution to movement. For example, in P<sub>1</sub> isolates, MSxx sometimes moves not only to the Ea/Ep boundary but also beyond this point (data not shown), and beads on the ventral surface of MSxx move in the direction of cell movement (Fig. 8), suggesting that MSxx might be rolling in this direction, perhaps driven by cell-cell adhesion. This does not appear to occur in P<sub>4</sub>, as P<sub>4</sub> never passes the Ea/Ep boundary in P<sub>1</sub> isolates (data not shown).

Although many mechanisms may contribute to *C. elegans* gastrulation, other potentially redundant mechanisms can be excluded by our results. First, our cell manipulation experiments suggest that neighboring cells do not chemotax towards each other. Second, the cells most likely do not move by protrusion-based cell crawling, as no protrusive structures were observed during gastrulation, and surfaces do not move in the directions expected in protrusion-based cell crawling. Thus, *C. elegans* gastrulation could be used as a model to examine cell motility that is not dependent on cell protrusions.

Additionally, because the descendants of P<sub>1</sub> isolates can gastrulate in vitro, we conclude that at least three classes of mechanisms for cell positioning are not essential for gastrulation movements, although the possibility that they make redundant or additive contributions to movements cannot be discounted. First, buckling forces or spatial restriction of cell divisions requiring physical constraints, such as those provided by the eggshell and vitelline envelope, cannot be

necessary for gastrulation because gastrulation can occur in devitellinized embryos. For example, the P<sub>3</sub> division in intact embryos is aligned with the eggshell, so that when P<sub>4</sub> is born, it might push Ep towards the center of the embryo. However, oriented P<sub>3</sub> cell division constrained by the eggshell cannot be required to initiate gastrulation movements because gastrulation can occur *in vitro*.

Second, we can rule out the necessity of a neighbor annealing mechanism in which, as the neighboring cells (P<sub>4</sub>, MSpp, MSpa, MSap, ABplpa and ABplpp) converge on the ventral side of Ea and Ep (Fig. 1C), their adhesiveness to each other drives their convergence, sealing up the ventral cleft. As the AB cells are not required for gastrulation movements, and as movements can occur in P<sub>1</sub> isolate orientations in which the only neighboring cells, P<sub>4</sub> and MSxx, do not contact each other until the end of gastrulation movements (Fig. 2M-P), we conclude that neighbor annealing is not required for gastrulation.

Third, a model whereby movement is driven exclusively by differential adhesion between cells is unlikely. The differential adhesion hypothesis (Steinberg, 1963) proposes that cell rearrangements can be directed by differences in the adhesive strengths of cells. Cells that show some degree of motility tend to maximize adhesive contacts, resulting in the most adhesive cells ending up in the center of a group of cells, with the less adhesive cells surrounding them (Steinberg and Takeichi, 1994). For example, it is possible that Ea and Ep could be more adhesive than their neighbors, and this differential adhesion could drive their ingression as they become surrounded by their less adhesive neighbors. However, differential adhesion alone cannot be a sufficient mechanism as Ea and Ep in linear P<sub>1</sub> isolates exhibit gastrulation movements without being surrounded by neighboring cells. In addition, there is, to date, no evidence for a role for adhesion molecules in *C. elegans* gastrulation, as molecules such as catenins, cadherins and extracellular matrix components do not show upregulation in the E cells at the time of gastrulation, and embryos carrying mutations in genes that encode adhesion proteins do not arrest until late embryogenesis, during the events of ventral closure and elongation (reviewed by Michaux et al., 2001). However, large-scale knockouts of adhesion molecules have not been performed, and functional redundancy may have prevented a gastrulation phenotype from being detected thus far.

### Cell contraction in morphogenesis

Our model of ventral contraction (Fig. 10) is reminiscent of apical constriction, a long-proposed mechanism for certain morphogenetic events. Cells that contract at their apical sides basolaterally expand, which in a cell sheet can cause bending or invagination of the sheet at the site of the apically constricting cells (Lewis, 1947; Odell et al., 1981). Because of their shape, these cells are often described as flask or bottle cells (Rhumbler, 1899; Rhumbler, 1902; Ruffini, 1925). Apical constriction has been suggested to play a role in morphogenetic movements in a wide range of organisms, including gastrulation in shrimp (Hertzler and Clark, 1992), fly (Young et al., 1991), jellyfish (Byrum, 2001), sea urchin (Kimberly and Hardin, 1998), white sturgeon (Bolker, 1993), rabbit (Viebahn et al., 1995) and frog (Keller, 1981; Hardin and Keller, 1988), as well as in primitive streak formation in chick and rat

embryos (Solursh and Revel, 1978), and neurulation in frogs (Jacobson et al., 1986). Whether apical constriction actually drives shape changes in cell sheets has been directly tested in *Xenopus*, sea urchin and *Drosophila* gastrulation. In *Xenopus* and sea urchin embryos, removal or ablation of bottle cells showed that the initial invagination of the epithelial sheet required the bottle cells (Keller, 1981; Hardin and Keller, 1988; Kimberly and Hardin, 1998). The cellular mechanism by which bottle cells invaginate is unclear. In *Drosophila* embryos, myosin and actin are enriched at the apical cortex of gastrulating cells (Young et al., 1991). In addition, disrupting a pathway that regulates actin through RhoA prevents concerted apical constriction, halting gastrulation (Barrett et al., 1997; Hacker and Perrimon, 1998). However, some clusters of cells still undergo apical constriction, suggesting that this pathway is required for concerted cell shape changes, but not for apical constriction.

The apical constriction model predicts a local actomyosin-driven cell contraction (Odell et al., 1981). Our results demonstrate that *C. elegans* gastrulation is an example of apical constriction. We define the apical and basal sides of cells based on findings by Nance and Priess (Nance and Priess, 2002) that cell cortices facing the outside of the embryo, or apical side, have an enrichment of the protein PAR-3. NMY-2 also accumulates at the apical side (Nance and Priess, 2002) and we show, through pharmacological studies, that both actin and myosin activity are required for gastrulation. Furthermore, the apical surfaces of Ea and Ep contract, and the polarity of Ea and Ep is important for the direction of movement by their neighbors. As adherens junctions and tight junctions are not found this early in embryogenesis (Krieg et al., 1978), we conclude that apical constriction can function to position blastomeres in early embryos, even before such cell-cell junctions form. The availability of both genetic tools and direct manipulation of cells should contribute to the usefulness of *C. elegans* as a system for understanding the mechanism of apical constriction in early embryos.

We thank Bruce Bowerman, Karen Oegema, Tony Hyman, Christian Malone and Ken Kemphues for strains; Sharon Milgram and Ted Salmon for antibodies and reagents; Victoria Madden, Robert Bagnell and Tony Perdue for SEM and confocal assistance; Jeff Molk, Julie Canman, Dale Beach, Rebecca Cheeks and Bill Mohler for imaging assistance and advice; and Kerry Bloom and his laboratory for generous use of their microscope setup. Some strains used in this work were provided by the *Caenorhabditis* Genetics Center, which is funded by the National Center for Research Resources of the NIH. J. L. thanks Nathan Hall for statistical analysis and moral support. We especially thank Mark Peifer, Jean-Claude Labbé, Mythreye Karthikeyan and Nate Dudley for critical reading of the manuscript, as well as members of the Goldstein laboratory and Ray Keller for helpful discussions. This work was supported by a March of Dimes Basil O'Connor Starter Scholar Award to B.G., who is a Pew Scholar in the Biomedical Sciences.

### REFERENCES

- Babu, P. (1974). Biochemical genetics of *Caenorhabditis elegans*. *Mol. Gen. Genet.* **135**, 39-44.
- Barrett, K., Leptin, M. and Settleman, J. (1997). The Rho GTPase and a putative RhoGEF mediate a signaling pathway for the cell shape changes in *Drosophila* gastrulation. *Cell* **91**, 905-915.

- Bei, Y., Hogan, J., Berkowitz, L. A., Soto, M., Rocheleau, C. E., Pang, K. M., Collins, J. and Mello, C. C. (2002). SRC-1 and Wnt signaling act together to specify endoderm and to control cleavage orientation in early *C. elegans* embryos. *Dev. Cell* **3**, 113-125.
- Berkowitz, L. A. and Strome, S. (2000). MES-1, a protein required for unequal divisions of the germline in early *C. elegans* embryos, resembles receptor tyrosine kinases and is localized to the boundary between the germline and gut cells. *Development* **127**, 4419-4431.
- Bolker, J. A. (1993). Gastrulation and mesoderm morphogenesis in the white sturgeon. *J. Exp. Zool.* **266**, 116-131.
- Boyd, L., Guo, S., Levitan, D., Stinchcomb, D. T. and Kemphues, K. J. (1996). PAR-2 is asymmetrically distributed and promotes association of P granules and PAR-1 with the cortex in *C. elegans* embryos. *Development* **122**, 3075-3084.
- Brenner, S. (1974). The genetics of *Caenorhabditis elegans*. *Genetics* **77**, 71-94.
- Byrum, C. A. (2001). An analysis of hydrozoan gastrulation by unipolar ingression. *Dev. Biol.* **240**, 627-640.
- Edgar, L. G. (1995). Blastomere culture and analysis. *Methods Cell Biol.* **48**, 303-321.
- Ettensohn, C. A. (1991). Primary mesenchyme cell migration in the sea urchin embryo. In *Gastrulation: Movements, Patterns, and Molecules* (ed. R. Keller, W. H. Clark, Jr and F. Griffin), pp. 289-304. New York: Plenum Press.
- Goldstein, B. (1992). Induction of gut in *Caenorhabditis elegans* embryos. *Nature* **357**, 255-257.
- Goldstein, B. (1995). Cell contacts orient some cell division axes in the *Caenorhabditis elegans* embryo. *J. Cell Biol.* **129**, 1071-1080.
- Guo, S. and Kemphues, K. J. (1996). A non-muscle myosin required for embryonic polarity in *Caenorhabditis elegans*. *Nature* **382**, 455-458.
- Hacker, U. and Perrimon, N. (1998). DRhoGEF2 encodes a member of the Dbl family of oncogenes and controls cell shape changes during gastrulation in *Drosophila*. *Genes Dev.* **12**, 274-284.
- Hardin, J. and Keller, R. (1988). The behaviour and function of bottle cells during gastrulation of *Xenopus laevis*. *Development* **103**, 211-230.
- Hertzler, P. L. and Clark, W. H., Jr (1992). Cleavage and gastrulation in the shrimp *Sicyonia ingentis*: invagination is accompanied by oriented cell division. *Development* **116**, 127-140.
- Italiano, J. E., Jr, Roberts, T. M., Stewart, M. and Fontana, C. A. (1996). Reconstitution in vitro of the motile apparatus from the amoeboid sperm of *Ascaris* shows that filament assembly and bundling move membranes. *Cell* **84**, 105-114.
- Jacinto, A., Martinez-Arias, A. and Martin, P. (2001). Mechanisms of epithelial fusion and repair. *Nat. Cell Biol.* **3**, E117-E123.
- Jacobson, A. G., Oster, G. F., Odell, G. M. and Cheng, L. Y. (1986). Neurulation and the cortical tractor model for epithelial folding. *J. Embryol. Exp. Morphol.* **96**, 19-49.
- Keller, R., Clark, W. H. J. and Griffin, F. (1991). *Gastrulation: Movements, Patterns, and Molecules*. New York: Plenum Press.
- Keller, R. E. (1981). An experimental analysis of the role of bottle cells and the deep marginal zone in gastrulation of *Xenopus laevis*. *J. Exp. Zool.* **216**, 81-101.
- Kimberly, E. L. and Hardin, J. (1998). Bottle cells are required for the initiation of primary invagination in the sea urchin embryo. *Dev. Biol.* **204**, 235-250.
- Knight, J. K. and Wood, W. B. (1998). Gastrulation initiation in *Caenorhabditis elegans* requires the function of gad-1, which encodes a protein with WD repeats. *Dev. Biol.* **198**, 253-265.
- Krieg, C., Cole, T., Deppe, U., Schierenberg, E., Schmitt, D., Yoder, B. and von Ehrenstein, G. (1978). The cellular anatomy of embryos of the nematode *Caenorhabditis elegans*. Analysis and reconstruction of serial section electron micrographs. *Dev. Biol.* **65**, 193-215.
- Lauffer, J. S., Bazzicalupo, P. and Wood, W. B. (1980). Segregation of developmental potential in early embryos of *Caenorhabditis elegans*. *Cell* **19**, 569-577.
- Lewis, W. (1947). Mechanics of invagination. *Anat. Rec.* **97**, 139-156.
- Lin, R., Hill, R. J. and Priess, J. R. (1998). POP-1 and anterior-posterior fate decisions in *C. elegans* embryos. *Cell* **92**, 229-239.
- Mabuchi, I. and Takano Ohmuro, H. (1998). Effects of inhibitors of myosin light chain kinase and other protein kinases on the first cell division of sea urchin eggs. *Dev. Growth Differ.* **32**, 549-556.
- Maduro, M. F. and Rothman, J. H. (2002). Making worm guts: the gene regulatory network of the *Caenorhabditis elegans* endoderm. *Dev. Biol.* **246**, 68-85.
- Michaux, G., Legouis, R. and Labouesse, M. (2001). Epithelial biology: lessons from *Caenorhabditis elegans*. *Gene* **277**, 83-100.
- Mitchison, T. J. and Cramer, L. P. (1996). Actin-based cell motility and cell locomotion. *Cell* **84**, 371-379.
- Munro, E. M. and Odell, G. M. (2002). Polarized basolateral cell motility underlies invagination and convergent extension of the ascidian notochord. *Development* **129**, 13-24.
- Nance, J. and Priess, J. R. (2002). Cell polarity and gastrulation in *C. elegans*. *Development* **129**, 387-397.
- Odell, G. M., Oster, G., Alberch, P. and Burnside, B. (1981). The mechanical basis of morphogenesis. I. Epithelial folding and invagination. *Dev. Biol.* **85**, 446-462.
- Oegema, K., Desai, A., Rybina, S., Kirkham, M. and Hyman, A. A. (2001). Functional analysis of kinetochore assembly in *Caenorhabditis elegans*. *J. Cell Biol.* **153**, 1209-1226.
- Priess, J. R. and Hirsh, D. I. (1986). *Caenorhabditis elegans* morphogenesis: the role of the cytoskeleton in elongation of the embryo. *Dev. Biol.* **117**, 156-173.
- Rhumbler, L. (1899). Physikalische Analyse von Lebenserscheinungen der Zelle; III. *Arch. f. Entw. Mech.* **9**, 63.
- Rhumbler, L. (1902). Zur Mechanik des Gastrulationsvorganges, insbesondere der Invagination. Eine entwicklungsmechanische Studie. *Wilhelm Roux' Arch. Entw. Org.* **14**, 401-476.
- Rocheleau, C. E., Downs, W. D., Lin, R., Wittmann, C., Bei, Y., Cha, Y. H., Ali, M., Priess, J. R. and Mello, C. C. (1997). Wnt signaling and an APC-related gene specify endoderm in early *C. elegans* embryos. *Cell* **90**, 707-716.
- Ruchhoeft, M. L. and Harris, W. A. (1997). Myosin functions in *Xenopus* retinal ganglion cell growth cone motility in vivo. *J. Neurobiol.* **32**, 567-578.
- Ruffini, A. (1925). *Fisiogenia*. Milano: Francesco Vallardi.
- Saitoh, M., Ishikawa, T., Matsushima, S., Naka, M. and Hidaka, H. (1987). Selective inhibition of catalytic activity of smooth muscle myosin light chain kinase. *J. Biol. Chem.* **262**, 7796-7801.
- Schierenberg, E. and Junkersdorf, B. (1992). The role of eggshell and underlying vitelline membrane for normal pattern formation in the early *Caenorhabditis elegans* embryo. *Roux's Arch. Dev. Biol.* **202**, 10-16.
- Schierenberg, E., Miwa, J. and von Ehrenstein, G. (1980). Cell lineages and developmental defects of temperature-sensitive embryonic arrest mutants in *Caenorhabditis elegans*. *Dev. Biol.* **76**, 141-159.
- Schoenwolf, G. C. (1991). Cell movements in the epiblast during gastrulation and neurulation in avian embryos. In *Gastrulation: Movements, Patterns, and Molecules* (ed. R. Keller, W. H. Clark, Jr and F. Griffin), pp. 1-28. New York: Plenum Press.
- Shelton, C. A. and Bowerman, B. (1996). Time-dependent responses to glp-1-mediated inductions in early *C. elegans* embryos. *Development* **122**, 2043-2050.
- Shi, Y. and Mello, C. (1998). A CBP/p300 homolog specifies multiple differentiation pathways in *Caenorhabditis elegans*. *Genes Dev.* **12**, 943-955.
- Solursh, M. and Revel, J. P. (1978). A scanning electron microscope study of cell shape and cell appendages in the primitive streak region of the rat and chick embryo. *Differentiation* **11**, 185-190.
- Steinberg, M. S. (1963). Reconstitution of tissues by dissociated cells. *Science* **141**, 401-408.
- Steinberg, M. S. and Takeichi, M. (1994). Experimental specification of cell sorting, tissue spreading, and specific spatial patterning by quantitative differences in cadherin expression. *Proc. Natl. Acad. Sci. USA* **91**, 206-209.
- Sulston, J. E., Schierenberg, E., White, J. G. and Thomson, J. N. (1983). The embryonic cell lineage of the nematode *Caenorhabditis elegans*. *Dev. Biol.* **100**, 64-119.
- Tabara, H., Hill, R. J., Mello, C. C., Priess, J. R. and Kohara, Y. (1999). pos-1 encodes a cytoplasmic zinc-finger protein essential for germline specification in *C. elegans*. *Development* **126**, 1-11.
- Thorpe, C. J., Schlesinger, A., Carter, J. C. and Bowerman, B. (1997). Wnt signaling polarizes an early *C. elegans* blastomere to distinguish endoderm from mesoderm. *Cell* **90**, 695-705.
- Viebahn, C., Mayer, B. and Miething, A. (1995). Morphology of incipient mesoderm formation in the rabbit embryo: a light- and retrospective electron-microscopic study. *Acta Anat.* **154**, 99-110.
- Wang, Y. L., Silverman, J. D. and Cao, L. G. (1994). Single particle tracking of surface receptor movement during cell division. *J. Cell Biol.* **127**, 963-971.
- Wilson, P. and Keller, R. (1991). Cell rearrangement during gastrulation of

- Xenopus: direct observation of cultured explants. *Development* **112**, 289-300.
- Wood, W. B.** (1988). *The Nematode Caenorhabditis elegans*. Cold Spring Harbor: Cold Spring Harbor Laboratory Press.
- Wu, D. Y. and Goldberg, D. J.** (1993). Regulated tyrosine phosphorylation at the tips of growth cone filopodia. *J. Cell Biol.* **123**, 653-664.
- Young, P. E., Pesacreta, T. C. and Kiehart, D. P.** (1991). Dynamic changes in the distribution of cytoplasmic myosin during *Drosophila* embryogenesis. *Development* **111**, 1-14.
- Yvon, A. M., Wadsworth, P. and Jordan, M. A.** (1999). Taxol suppresses dynamics of individual microtubules in living human tumor cells. *Mol. Biol. Cell* **10**, 947-959.
- Zar, J. H.** (1999). *Biostatistical Analysis*. Upper Saddle River, NJ: Prentice Hall.
- Zhu, J., Hill, R. J., Heid, P. J., Fukuyama, M., Sugimoto, A., Priess, J. R. and Rothman, J. H.** (1997). end-1 encodes an apparent GATA factor that specifies the endoderm precursor in *Caenorhabditis elegans* embryos. *Genes Dev.* **11**, 2883-2896.